

# A Data-Driven Stackelberg Market Strategy for Demand Response-Enabled Distribution Systems

Tianguang Lu, *Student Member, IEEE*, Zhaoyu Wang<sup>ID</sup>, *Member, IEEE*, Jianhui Wang<sup>ID</sup>, *Senior Member, IEEE*, Qian Ai, *Senior Member, IEEE*, and Chong Wang<sup>ID</sup>, *Member, IEEE*

**Abstract**—A data-based Stackelberg market strategy for a distribution market operator (DMO) is proposed to coordinate power dispatch among different virtual power plants, i.e., demand response (DR) aggregators (DRAs). The proposed strategy has a two-stage framework. In the first stage, a data-driven method based on noisy inverse optimization estimates the complicated price-response characteristics of customer loads. The estimated load information of the DRAs is delivered to the second stage, where a one-leader multiple-follower stochastic Stackelberg game is formulated to represent the practical market interaction between the DMO and the DRAs that considers the uncertainty of renewables and the operational security. The proposed data-driven game model is solved by a new penalty algorithm and a customized distributed hybrid dual decomposition-gradient descent algorithm. Case studies on a practical DR project in China and a distribution test system demonstrate the effectiveness of the proposed methodology.

**Index Terms**—Market strategy, demand response, noisy inverse optimization, Stackelberg game, Lagrange dual decomposition.

## NOMENCLATURE

### Indices and Sets

$\Omega_N$	Set of buses
$\Omega_L$	Set of lines
$\Omega_D/\Omega_i$	Strategy set of DMO/aggregator $i$
$t$	Time index $t \in \mathcal{T}$
$i$	Aggregator index $i \in \mathcal{I}$
$s$	Scenario index $s \in \mathcal{S}$
$q$	Iteration index
$\mathcal{T}$	Set of $t$
$\mathcal{I}$	Set of $i$
$\mathcal{S}$	Set of $s$

Manuscript received April 20, 2017; revised August 19, 2017 and November 16, 2017; accepted January 11, 2018. This work was supported in part by the National Natural Science Foundation of China under Grant 51577115 and Grant U1766207, and in part by the U.S. Department of Energy Office of Electricity Delivery and Energy Reliability under Contract DE-OE0000839. Paper no. TSG-00535-2017. (*Corresponding author: Zhaoyu Wang.*)

T. Lu and Q. Ai are with Shanghai Jiao Tong University, Shanghai 200240, China (e-mail: ltghao@163.com; aiqian@sjtu.edu.cn).

Z. Wang and C. Wang are with Iowa State University, Ames, IA 50011 USA (e-mail: wzy@iastate.edu; wangc@iastate.edu).

J. Wang is with the Department of Electrical Engineering, Southern Methodist University, Dallas, TX 75275 USA, and also with the Energy Systems Division, Argonne National Laboratory, Argonne, IL, USA (e-mail: jianhui.wang@ieee.org).

Color versions of one or more of the figures in this paper are available online at <http://ieeexplore.ieee.org>.

Digital Object Identifier 10.1109/TSG.2018.2795007

$n, m, k$	Integer indices	32
$G$	Normal form of Stackelberg game	33
$C_i$	Price signal set of aggregator $i$	34
$\Omega_C$	Price signal set of all aggregators	35
$\mathcal{P}_i$	Consumption set of aggregator $i$	36
$\Omega_P$	Consumption set of all aggregators	37
$\Omega_R$	Variable set of penalty algorithm.	38

### Parameters

$c_{i,t}^h$	Historical price data of aggregator $i$ at time $t$	40
$\omega_t$	Weight of absolute values at time $t$	41
$x_{i,t}^h$	Historical consumption data of aggregator $i$ at time $t$	42
$M$	Penalty factor of the reformulation	44
$F$	Forgetting factor	45
$p_{n,t}^d/q_{n,t}^d$	Demand active/reactive power at bus $n \in \Omega_N, n \notin \mathcal{I}$	46
$c^g$	Generation cost of DG $g$	48
$\bar{p}^g$	Maximum generation of DG $g$	49
$p_{i,t}^{r,s}$	Renewable generation of aggregator $i$ at time $t$ in scenario $s$	50
$c_t$	Electricity prices set by ISO at time $t$	52
$\bar{g}_t$	Planned purchased electricity set by ISO at time $t$	53
$\bar{p}_i^d/\bar{q}_i^d$	Maximum active/reactive exchange power at bus connected to aggregator $i$	55
$\bar{P}_{nm}/\bar{Q}_{nm}$	Active/reactive power limit of line $(n, m)$	57
$\bar{c}$	Maximum electricity price set by DMO	58
$b_n^1/b_n^2$	Resistance/reactance between buses $n$ and $n+1$	59
$\mu$	Power redispatch cost	60
$\varepsilon$	Voltage deviation	61
$\gamma_t$	Price penalty paid for mismatch between energy generation and consumption	62
$T$	Total number of samples	64
$N$	Proportion of different samples	65
$r_{i,t}^{g,u}/r_{i,t}^{g,d}$	Pick-up/drop-off rate of DGs	66
$Pr(s)$	Probability of realization for $s \in \mathcal{S}$	67
$\mathbb{E}_s$	Expectation with respect to $\mathcal{S}$	68
$K$	Number of concatenated elements.	69

### Variables

$\mathcal{Q}(p)$	Second-stage stochastic problem	71
$\Delta p_{i,t}^s$	Mismatch variable	72
$\phi(p, s)$	Mismatch problem	73

74	$\mathbf{c}_1, \mathbf{c}_2, \mathbf{p}_1, \mathbf{p}_2,$	Compact notations of primary problem
75	$\mathbf{A}_1, \mathbf{A}_2, \mathbf{b}_1, \mathbf{b}_2,$	
76	$\mathcal{P}, \mathcal{Q}(\mathbf{R}), f(\mathbf{g})$	
77	$L(\cdot)$	Lagrangian form
78	$\tilde{P}_{i,t}^l, \tilde{P}_{i,t}^g$	Stackelberg equilibrium variables
79	$p_k, c_k, \mathbf{u}_1, \mathbf{u}_2,$	Dual decomposition notations
80	$\mathbf{A}_k, \mathbf{u}_k, \kappa, \mathbf{c}'_k,$	
81	$\delta_1, \delta_2$	
82	$u_{i,t}^1, u_{i,t}^2$	Lagrange multipliers of aggregator $i$ at time $t$
83		
84	$\theta_{i,t}$	Parameter vector of price response in aggregator $i$ at time $t$
85		
86	$x_{i,t}$	Power consumption of aggregator $i$ at time $t$ in data-driven stage
87		
88	$\lambda_{i,t}^u, \lambda_{i,t}^d$	Dual variables of rate constraints of aggregator $i$ at time $t$
89		
90	$\underline{\psi}_{i,t}, \overline{\psi}_{i,t}$	Dual variables of limit constraints of aggregator $i$ at time $t$
91		
92	$\alpha_{i,t}^+, \alpha_{i,t}^-$	Auxiliary variables to reformulate the absolute value
93		
94	$a_{i,t}$	Marginal utility of aggregator $i$ at time $t$
95	$\overline{P}_{i,t}/\underline{P}_{i,t}$	Maximum/minimum consumption of aggregator $i$ at time $t$
96		
97	$r_{i,t}^u/r_{i,t}^d$	Maximum consumption pick-up/drop-off of aggregator $i$ at time $t$
98		
99	$p_{i,t}^d$	Power exchange at bus connected to aggregator $i$ at time $t$
100		
101	$p_{i,t}^l$	Customer consumption of aggregator $i$ at time $t$ in Stackelberg-pricing stage
102		
103	$P_{i,t}^g$	DG generation of aggregator $i$ at time $t$
104	$c_{i,t}^l$	Electricity price of aggregator $i$ set by DMO at time $t$
105		
106	$g_t$	Electricity purchased from wholesale market at time $t$
107		
108	$P_{n,t}/Q_{n,t}$	Active/reactive power flow from bus $n$ to $n+1$ at time $t$
109		
110	$V_{n,t}$	Voltage magnitude at bus $n$ at time $t$
111	$U_D/U_i$	Utility function of DMO/aggregator $i$ .

## I. INTRODUCTION

THE GROWING demand for electricity, emerging smart houses, rapid growth of plug-in hybrid electric vehicles, and increasing installation of renewable distributed generators (DG) in distribution systems bring unprecedented challenges to utilities, end users, and other participants in retail markets [1], [2]. To solve these challenges, new distribution-level market strategies are needed to bridge the regulation gap between the wholesale market and end participants in distribution systems. Demand response (DR), which aims to exploit inherent demand-side flexibility [3], [4], is regarded as an effective and promising approach to distribution-level market operation. Price-based DR programs utilize dynamic price signals to influence consumption patterns according to each customers' usage tendencies. A fundamental challenge for price-based DR is how to model customer reactions to electricity prices. In [5], the price-elasticity pattern was modeled as a bilinear function, with electricity price and energy consumption as variables to

simplify the computation. Reference [6] proposed a hierarchical price-elasticity model to maximize the profits of virtual power plants (VPP) and end users. Customer dissatisfaction was considered in the optimization as a quadratic function with a fixed consumption point, where the dissatisfaction increased as consumption deviated from this point. The work in [7] introduced a reward mechanism for residential customers to shave peak loads. The customer consumption characteristics were captured by survey questionnaires, which can provide useful information but are time-consuming, inaccurate, and unadaptive. Most existing methods model price-consumption characteristics based on experiences and hypotheses, where a certain price leads to a specific consumption level. However, these assumed models cannot represent the diversified, operation condition-based, and time-varying price responses [8] that exist in today's distribution systems. Moreover, some price-response models are based on complicated polynomial or exponential forms, which increases the computational difficulty when applying these algorithms [9]. The growing implementation of advanced metering infrastructure (AMI) provides a new opportunity to learn and capture the price-responsive patterns of customers via data-driven methods.

Data-oriented modeling approaches of price-demand elasticity have drawn considerable attention in recent DR research. Reference [10] introduced a Gaussian process to model the response of building energy consumption to price signals. In [11], a quantile regression non-parametric model was developed to decide pricing strategies based on probability distributions of historical consumption data. A convex optimization problem scalable to very big datasets was formulated to model the relationship between day-ahead prices and customer response. The study in [12] proposed an extended version of a stacked denoising autoencoder model to represent the hourly price elasticity pattern of industrial users. A deep neural network was utilized in the model to improve the forecasting performance. However, all of the mentioned studies only offer forecasting methods without considering their application to DR programs.

One key issue for demand-side resources is their relatively small individual capacities. A second key issue is that their degree of flexibility can depend on local environmental conditions and the local objectives of their owners or managers. Harnessing useful service flexibility from these resources thus requires some form of aggregation of their service capabilities, which increases the effective capacity of the resulting aggregated resource to achieve dispatchability through an averaging of local conditions. A demand response aggregator (DRA) or a virtual power plant (VPP) serves this purpose.

Recently, there has been much interest in adopting the Stackelberg game to build hierarchical models for practical decision-making problems in power markets [13]. A bilevel game between power service providers and users was proposed in a retail market [14]. This model aimed to assist providers to set optimal strategies and encourage users to adjust their power usage. Reference [15] presented a real-time DR algorithm based on the Stackelberg game to control smart appliances. A virtual electricity trading process was designed to balance local objectives between followers (devices) and the

188 leader (energy management center). In [13], a Stackelberg-  
 189 based time-of-use electricity pricing strategy was introduced  
 190 to a DR program. Optimal prices were set to control elec-  
 191 tricity demand while considering user satisfaction. In [16],  
 192 the energy trading between prosumers and a power company  
 193 was studied through a non-cooperative Stackelberg model.  
 194 Particularly, the expected profits of the prosumers were max-  
 195 imized by a unique pure-strategy Nash equilibrium under  
 196 classical game theory. An energy-aware resource allocation  
 197 scheme was proposed in [17] using a Stackelberg game for  
 198 energy management in cloud-based data centers. In [18], a  
 199 demand response problem was presented in a smart grid  
 200 consisting of a retailer and multiple residential consumers,  
 201 where the real-time pricing and aggregate cost were opti-  
 202 mized through an adaptive diffusion algorithm. To obtain a  
 203 unique Stackelberg equilibrium, most existing papers (such  
 204 as [13]–[15]) simplify their market models by only consid-  
 205 ering fixed upper and lower bounds of demand-side consump-  
 206 tion or generation, which lacks authenticity and comprehensiv-  
 207 ness. In addition, operation constraints such as power flows  
 208 and voltage deviations are ignored in most Stackelberg game  
 209 models (such as [16], [19], and [20]) due to the computa-  
 210 tional complexity. In contrast, the proposed approach in this paper  
 211 builds a comprehensive market model using operational con-  
 212 straints and obtains a unique Stackelberg equilibrium through  
 213 a distributed Lagrange decomposition algorithm. Furthermore,  
 214 most models (such as [17] and [18]) do not consider the uncer-  
 215 tainties of renewables, while these uncertainties are included  
 216 in the proposed Stackelberg model by leveraging the stochastic  
 217 programming.

218 To deal with the above-mentioned limitations, in this work  
 219 we formulate a data-driven Stackelberg game for the distri-  
 220 bution market. The proposed market strategy is a two-stage  
 221 framework with bilevel programming models in each stage.  
 222 In the first stage, the noisy data-based inverse scheme is  
 223 designed to perform a data-driven modeling of price responses.  
 224 In the second stage, the market strategy is modeled using a  
 225 Stackelberg game, which is reformulated as a bilevel stochas-  
 226 tic programming to characterize interactions between the utility  
 227 and DRAs with renewable energy.

228 As an effective state estimator, the inverse optimization  
 229 framework has been widely used in a variety of research  
 230 areas [21]–[23]. In this paper, the proposed data-driven method  
 231 is based on the inverse optimization scheme with two major  
 232 modifications. First, the training dataset is considered as a  
 233 known state vector and the estimator is based on customer  
 234 electricity consumption behavior. Second, a penalty factor  $M$   
 235 is used to minimize the out-of-sample prediction error.

236 The key contributions of this paper are threefold:

237 1) An innovative data-driven model is designed to estimate  
 238 demand-side flexibility via historical price-consumption data.  
 239 This model avoids the complexity of traditional load modeling,  
 240 guarantees the execution of user response under optimized  
 241 prices, and reduces computational burden. Moreover, the  
 242 inverse optimization algorithm in this paper is different from  
 243 conventional ones as it is based on noisy data, which not only  
 244 estimates price-response parameters but also minimizes their  
 245 prediction errors.

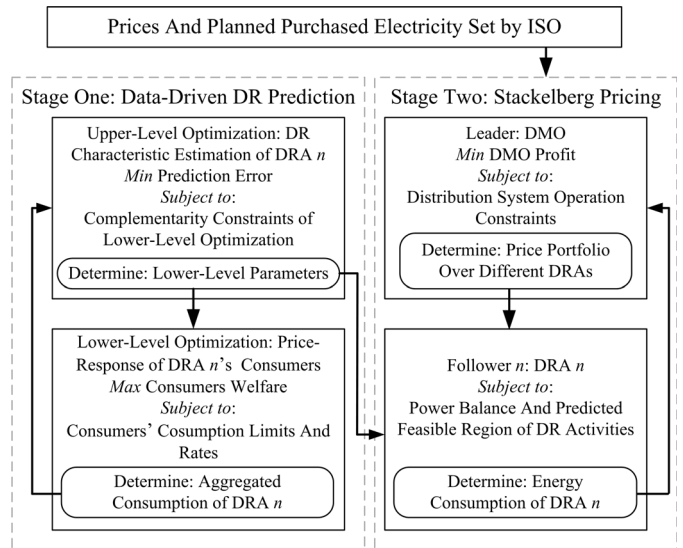


Fig. 1. Hierarchical architecture of the proposed strategy.

AQ3

2) The proposed Stackelberg game-based market strategy  
 246 considers market information from the independent system  
 247 operator (ISO), the operation security constraints, and the  
 248 stochasticity of distributed renewable generators. The proposed  
 249 distribution-level regulation model can directly fit into ISOs’  
 250 day-ahead/real-time wholesale markets and end participants in  
 251 retail markets, and bridge the gap between wholesale markets  
 252 and end participants.  
 253

3) Two customized algorithms are applied: one is a tuned  
 254 penalty algorithm with fast computation that precisely predicts  
 255 customers’ DR responses based on a large amount of historical  
 256 data; the other is a distributed hybrid dual decomposition-  
 257 gradient descent (HDDGD) algorithm that caters to the dis-  
 258 tributed market structure and converges to the optimal solution  
 259 of the Stackelberg game through efficient parallel computation.  
 260

The proposed methods are validated in a test case and  
 261 simulation using real DR data.  
 262

The rest of this paper is organized as follows. Section II  
 263 introduces the proposed market strategy architecture. The  
 264 first and second stage problem formulations are presented  
 265 in Sections III and IV, respectively. Solution algorithms are  
 266 implemented in Section V. Section VI analyzes numerical  
 267 results, followed by concluding remarks in Section VII.  
 268

## 269 II. PROPOSED MARKET-BASED FRAMEWORK

270 We assume that one distribution system consists of one dis-  
 271 tribution market operator (DMO) and multiple DRAs [24]. A  
 272 DRA, which includes a cluster of customer loads and DGs, can  
 273 access the aggregated load data of its own cluster. However,  
 274 it cannot access the information of other DRAs. DRAs com-  
 275 pete with each other on behalf of their customers, while the  
 276 DMO [25] leverages price signals to coordinate the utility  
 277 company and different DRAs.

278 Fig. 1 depicts the proposed two-stage hierarchical frame-  
 279 work consisting of a data-driven stage and a Stackelberg-  
 280 pricing stage. The first stage is based on an inverse  
 281 optimization scheme that leads to a bilevel optimization

282 problem for each DRA. The upper level utilizes historical  
 283 price-consumption data to estimate load ramp rates and con-  
 284 sumption limits subject to the price response models in the  
 285 lower level. The estimated parameters are then delivered to the  
 286 DRA (follower) of the Stackelberg game model. In the second  
 287 stage, the DRA uses stochastic programming to minimize the  
 288 costs of its aggregated energy consumption, unbalanced power,  
 289 and controllable DG generation. According to the expected  
 290 wholesale market information from the ISO, network opera-  
 291 tion constraints, and the expected consumption of DRAs, the  
 292 DMO (leader) calculates a pricing strategy for the DRAs and  
 293 the electricity that needs to be purchased from the wholesale  
 294 market. Through iterative interactions between the DMO and  
 295 DRAs, all players in the game reach an equilibrium.

### 296 III. STAGE ONE: DATA-DRIVEN DR PREDICTION

297 To capture DR characteristics and determine the correspond-  
 298 ing model parameters for a DRA, the training procedure in the  
 299 data-driven stage is cast as a bilevel programming problem.  
 300 The upper level is a parameter-estimation problem, where the  
 301 load parameters of the lower-level are evaluated to minimize  
 302 data prediction errors.

#### 303 A. Lower-Level Problem: Price Response 304 of a DRA's Consumers

305 The lower-level problem is formulated using the consump-  
 306 tion decisions of the DRA's consumers, where parameters  
 307  $\theta_{i,t}$  are determined by the upper-level optimization (this  
 308 optimization is described in Section III-B). In the noisy  
 309 inverse theory [26], the consumption decision model is given  
 310 by a parameter vector  $\theta_{i,t} = \{a_{i,t}, r_{i,t}^u, r_{i,t}^d, \bar{P}_{i,t}, \underline{P}_{i,t}\}$ , at time  
 311  $t \in \mathcal{T} \equiv \{t : t = 1 \dots T\}$ . Aggregated consumers of a  
 312 DRA behave as welfare-maximizing individuals, whose utility  
 313 function represents total economic benefits and customer satis-  
 314 faction. This means we can use the following model to mimic  
 315 the electricity consumption decision-making of the customers.  
 316 Compared to existing methods, there is no need to assume the  
 317 model empirically or hypothetically since the upper level eval-  
 318 uates  $\theta_{i,t}$  according to historical records and prediction errors.  
 319 For  $\forall i \in \mathcal{I}$ :

$$320 \max_{x_{i,t}} \sum_{t \in \mathcal{T}} (a_{i,t} x_{i,t} - c_{i,t}^h x_{i,t}) \quad (1a)$$

321 Let  $\mathcal{T}_{-1} = \{t : t = 2, \dots, T\}$ . The objective function is then  
 322 subject to:

$$323 x_{i,t} - x_{i,t-1} \leq r_{i,t}^u, t \in \mathcal{T}_{-1} \quad (1b)$$

$$324 x_{i,t-1} - x_{i,t} \leq r_{i,t}^d, t \in \mathcal{T}_{-1} \quad (1c)$$

$$325 x_{i,t} \leq \bar{P}_{i,t}, t \in \mathcal{T} \quad (1d)$$

$$326 x_{i,t} \geq \underline{P}_{i,t}, t \in \mathcal{T} \quad (1e)$$

327 Through load ramp rates and consumption limits, con-  
 328 straints (1b)–(1e) impose a feasible region on DR activi-  
 329 ties [27]. In addition, this feasible region and parameters in  
 330 the objective function change over time as customer behavior  
 331 is time variant. To recast the bilevel optimization problem in  
 332 the data-driven stage as a single-level problem, the following

Karush-Kuhn-Tucker (KKT) reformulations will be utilized in 333  
 the next subsection: 334

$$- \lambda_{i,2}^u + \lambda_{i,2}^d - \underline{\psi}_{i,1} + \bar{\psi}_{i,1} = a_{i,1} - c_{i,1}^h \quad (2a) \quad 335$$

$$a_{i,t} - c_{i,t}^h = \lambda_{i,t}^u - \lambda_{i,t+1}^u - \lambda_{i,t}^d + \lambda_{i,t+1}^d - \underline{\psi}_{i,t} + \bar{\psi}_{i,t}, \quad 336$$

$$t \in \mathcal{T}_{-1} \quad (2b) \quad 337$$

$$\lambda_{i,T}^u - \lambda_{i,T}^d - \underline{\psi}_{i,T} + \bar{\psi}_{i,T} = a_{i,T} - c_{i,T}^h \quad (2c) \quad 338$$

$$x_{i,t} - x_{i,t-1} \leq r_{i,t}^u \perp \lambda_{i,t}^u \geq 0, t \in \mathcal{T}_{-1} \quad (2d) \quad 339$$

$$x_{i,t-1} - x_{i,t} \leq r_{i,t}^d \perp \lambda_{i,t}^d \geq 0, t \in \mathcal{T}_{-1} \quad (2e) \quad 340$$

$$x_{i,t} \leq \bar{P}_{i,t} \perp \bar{\psi}_{i,t} \geq 0, t \in \mathcal{T} \quad (2f) \quad 341$$

$$\underline{P}_{i,t} \leq x_{i,t} \perp \underline{\psi}_{i,t} \geq 0, t \in \mathcal{T}_{-1}. \quad (2g) \quad 342$$

#### B. Upper-Level Problem: DR Characteristics Estimation 343

344 Given a time series of pairwise price-consumption data  
 345  $(c_{i,t}^h, x_{i,t}^h)$ , the inverse optimization estimates the value  
 346 of parameter vector  $\theta_{i,t}$ , which defines the lower-level  
 347 problem (1), such that the optimal solution of  $x_{i,t}$  resulting  
 348 from this problem is as close as possible to the historical data  
 349  $x_{i,t}^h$  in terms of a certain norm. The parameters in  $\theta_{i,t}$ , in turn,  
 350 best represent the price-response characteristics of aggrega-  
 351 tor  $i$ 's consumers. The mathematical formulation is described  
 352 below for  $\forall i \in \mathcal{I}$ : 352

$$\min_{x_{i,t}, \theta_{i,t}} \sum_{t \in \mathcal{T}} \omega_t |x_{i,t} - x_{i,t}^h| \quad (3a) \quad 353$$

$$s.t. \quad (2) \quad (3b) \quad 354$$

355 where constraints (3b) correspond to the KKT conditions of  
 356 lower-level problem (1). The variables  $\theta_{i,t}$  in (3), which repre-  
 357 sent the parameter vector in (1), are constrained by optimality  
 358 conditions, thus guaranteeing that  $x_{i,t}$  is optimal for (1). 358

359 The weight of the estimation error at time  $t$  is represented  
 360 by parameter  $\omega_t$  in (3a). These weights have a two-fold mean-  
 361 ing. For the day-ahead market, the weights represent the price  
 362 of the balancing power at time  $t$ . In this case, consumption at  
 363 time  $t$  with a higher balancing price matches the original data  
 364 better. For the real-time market,  $\omega_t = (t/T)^F$ , where param-  
 365 eter  $F$  indicates how rapidly the model forgets previous data.  
 366 To save computational costs and achieve faster convergence, a  
 367 forgetting factor  $F$  is integrated to apply exponentially decay-  
 368 ing weights to previous observations. As  $F (\geq 0)$  increases,  
 369 the weights of more recent observations become larger than  
 370 the old ones, and when  $F = 0$ , all observations are weighted  
 371 equally. The proposed data-driven method can be separately  
 372 applied to both the day-ahead scenario and the real-time  
 373 scenario. 373

374 To remove the absolute value sign, problem (3) can be reform-  
 375 ulated as the following linear objective function plus two  
 376 additional constraints for  $\forall i \in \mathcal{I}$ : 376

$$\min_{x_{i,t}, \theta_{i,t}, \alpha_{i,t}^+, \alpha_{i,t}^-} \sum_{t \in \mathcal{T}} \omega_t (\alpha_{i,t}^+ + \alpha_{i,t}^-) \quad (4a) \quad 377$$

$$s.t. \quad (2). \quad (4b) \quad 378$$

$$x_{i,t} - x_{i,t}^h = \alpha_{i,t}^+ - \alpha_{i,t}^-, t \in \mathcal{T} \quad (4c) \quad 379$$

$$\alpha_{i,t}^+, \alpha_{i,t}^- \geq 0, t \in \mathcal{T} \quad (4d) \quad 380$$

In summary, we established (1) to represent the parametric price-response model for DRA  $i$ 's flexible consumers. Compared to traditional load modeling that has polynomial, exponential, or other complicated forms, the proposed price-response model uses linear constraints (1b)–(1e) to precisely describe the feasible region of DR activities. The accuracy of the proposed model is ensured because time-varying parameters  $\theta_{i,t}$  are included in the linear constraints to represent the feasible region at time  $t$ , and estimation problem (4) is proposed to best estimate  $\theta_{i,t}$  by using the sum of the weighted absolute values of residuals, i.e., the measure of prediction errors. In addition, according to the theory of statistical learning, the predicted data set should have the same type of information as the training data set. Hence, to predict a certain type of operation, the training data must be based on the same type of price signals (e.g., the prediction of day-ahead operation is based on the training data resulting from day-ahead prices).

#### IV. STAGE TWO: STACKELBERG PRICING STRATEGY

A typical Stackelberg game provides a framework to model the problems wherein one player (leader) has the ability to enforce its strategy on the other player (follower). As an extension to the original single-follower Stackelberg game, a one-leader,  $n$ -follower game is presented in stage two to model the practical interaction between the DMO and non-cooperative DRAs.

A Stackelberg game is composed of players, the strategy sets of the players, and utility functions. The proposed game model is defined in its normal form as  $G = \{\Omega_D, \{\Omega_i\}_{i \in \mathcal{I}}; U_D, \{U_i\}_{i \in \mathcal{I}}\}$  [28], where the DMO acts as the leader and the DRAs act as followers. The leader's strategy is constituted by a time series of prices and purchased electricity from the wholesale market. Each follower's strategy includes its aggregated energy consumption and controllable DG outputs. The strategy set of each player is determined according to certain constraints. The utility functions are defined as the quantified benefits of the leader and its followers, respectively [15].

The proposed game is played in the following sequence. The leader first announces its strategy to the followers. Each follower then decides an optimal strategy as its best response to the leader's strategy and informs the leader of its best response. The leader then updates its strategy based on this feedback and announces its updated strategy. This interactive process is iterated until all players obtain their desired outcomes, i.e., a Stackelberg equilibrium (SE) is achieved, where the leader maximizes its benefit based on the identified best-response strategies of all followers. Thus, the SE can be expressed as a portfolio of equilibrium over strategy sets. Each player will not deviate from this equilibrium.

Thus, the proposed game model can be reformulated as a bilevel programming with the DMO in the upper level and the DRAs in the lower level. This approach is detailed in the following subsections.

#### A. Lower-Level Follower (DRA $i$ ) Model

For each follower, let  $C_i = [c_{i,1}^l, c_{i,2}^l, \dots, c_{i,T}^l]$  be the pricing strategy of DRA  $i$ , then  $\Omega_C = \{C_i : i \in \mathcal{I}\}$  is the pricing strategy of the DMO for all DRAs. We develop a two-stage stochastic formulation of DRA  $i$ 's utility function and strategy set below, that takes into consideration the uncertainty of any renewable DGs.

1) *The First-Stage Stochastic Problem:* When  $C_i$  is revealed to DRA  $i$ , the deterministic costs resulting from competing with other DRAs and interacting with the DMO includes two parts: the operational cost of its controllable DGs and the cost of purchasing electricity to meet aggregated power consumption. To minimize these costs, the formulation is:

$$\min_{p_{i,t}^l, p_{i,t}^g} -U_i = \sum_{t \in \mathcal{T}} (c_{i,t}^l p_{i,t}^l + c^g p_{i,t}^g) + Q(p) \quad (5a)$$

$$s.t. \quad p_{i,t}^l - p_{i,t-1}^l \leq r_{i,t}^u, t \in \mathcal{T}_{-1} \quad (5b)$$

$$p_{i,t-1}^l - p_{i,t}^l \leq r_{i,t}^d, t \in \mathcal{T}_{-1} \quad (5c)$$

$$p_{i,t}^l \leq \bar{P}_{i,t}, t \in \mathcal{T} \quad (5d)$$

$$p_{i,t}^l \geq \underline{P}_{i,t}, t \in \mathcal{T} \quad (5e)$$

$$p_{i,t}^g - p_{i,t-1}^g \leq r_{i,t}^{g,u}, t \in \mathcal{T}_{-1} \quad (5f)$$

$$p_{i,t-1}^g - p_{i,t}^g \leq r_{i,t}^{g,d}, t \in \mathcal{T}_{-1} \quad (5g)$$

$$0 \leq p_{i,t}^g \leq \bar{p}^g, t \in \mathcal{T} \quad (5h)$$

where

$$Q(p) = \mathbb{E}_s \phi(p, s) = \sum_{s \in \mathcal{S}} Pr(s) \phi(p, s) \quad (5i)$$

The objective function (5a) includes the first-stage cost and the second-stage expected cost. In Section III, load parameters such as ramp rates ( $r_{i,t}^u, r_{i,t}^d$ ) and power limits ( $\bar{P}_{i,t}, \underline{P}_{i,t}$ ) are used in constraints (5b)–(5e) and constitute the predicted feasible region of DR activities. However, these parameters cannot be directly applied because of potential data synchronization issues. The data training in (3) and the operations for the aggregators in (5) are usually in different time scales. For example, the data extraction in (3) might be performed every 15 min, while the operation in (5) might be hourly. We propose the following technique to deal with this asynchronization. Let index 0 and index 1 denote the original parameters and the applied parameters, respectively. When  $T^0 > T^1$ :

$$N = \lfloor T^0 / T^1 \rfloor \quad (6a)$$

$$\theta_{i,t}^1 = \frac{1}{N+1} \sum_{n=Nt^1-N}^{Nt^1+N} \theta_{i,n}^0, t^1 = 1, 2, \dots, T^1 \quad (6b)$$

When  $T^1 \geq T^0$ :

$$N = \lceil T^0 / T^1 \rceil \quad (6c)$$

$$\theta_{i,t}^1 = \theta_{i,t^0}^0, t \in (Nt^0 - N, Nt^0], t^0 = 1, 2, \dots, T^0. \quad (6d)$$

2) *The Second-Stage Stochastic Problem:* The second-stage problem is established after the energy consumption and controllable DG outputs are determined. The objective function of this stage is to minimize the penalty cost of the mismatch

481  $\Delta p_{i,t}^s$  caused by the stochastic nature of renewable energy  
482 generation.

$$483 \quad \phi(p, s) = \min \sum_{t \in \mathcal{T}} \gamma_t \Delta p_{i,t}^s \quad (7a)$$

$$484 \quad \Delta p_{i,t}^s = p_{i,t}^l - p_{i,t}^d - p_{i,t}^g - p_{i,t}^{r,s} \quad (7b)$$

485 Due to the continuity of the probability distributions, it is  
486 difficult to analytically address these uncertainties. To han-  
487 dle this difficulty, the sample average approximation (SAA)  
488 method is applied to generate a certain number of scenarios  
489 to represent the probability distribution of the random param-  
490 eters [29]. Therefore, (5i) can be replaced by its approximated  
491 form

$$492 \quad \mathcal{Q}(p) = \frac{1}{S} \sum_{s \in \mathcal{S}} \sum_{t \in \mathcal{T}} \gamma_t \Delta p_{i,t}^s \quad (8)$$

493 where the scenario set has  $S$  realizations of random variable  
494  $p_{i,t}^{r,s}$ . Studies have proved that the optimal solution of the reform-  
495 ulated problem (5) will converge to the original solution if  
496 a sufficient number of scenarios are performed [30]. Hence,  
497 the original stochastic problem can be reformulated as a con-  
498 tinuous deterministic optimization problem. Additionally, the  
499 feasible strategy set of aggregator  $i$  can be defined as

$$500 \quad \Omega_i = \left\{ p_{i,t}^g, p_{i,t}^l \mid (5b) - (5h), (7b), (8) \right\}. \quad (9)$$

### 501 B. Upper-Level Leader (DMO) Model

502 Let  $\mathcal{P}_i = [p_{i,1}^l, p_{i,2}^l, \dots, p_{i,T}^l]$  be the consumption strategy  
503 of DRA  $i$ , then  $\Omega_P = \{\mathcal{P}_i : i \in \mathcal{I}\}$  is the strategy profile  
504 containing all of the optimal strategies of its followers. When  
505 DRAs respond to the DMO with  $\Omega_P$ , the utility function of  
506 the leader can be defined as

$$507 \quad U_D = \sum_{i \in \mathcal{I}} \sum_{t \in \mathcal{T}} c_{i,t}^l p_{i,t}^l - \sum_{t \in \mathcal{T}} c_t g_t - \sum_{t \in \mathcal{T}} \mu (g_t - \bar{g}_t)^2 \quad (10)$$

508 The leader updates its strategy based on the followers'  
509 strategies, so the first term of (10) includes the benefit gained  
510 from the energy consumption of each DRA. The second term  
511 is the cost of purchasing electricity from the wholesale mar-  
512 ket. The third term is the cost of redispatching the purchased  
513 electricity, where the squared expression represents the redis-  
514 patched power. To maintain operational security, the following  
515 power flow and voltage constraints should be applied:

$$516 \quad P_{1,t} = g_t, t \in \mathcal{T} \quad (11a)$$

$$517 \quad P_{n+1,t} = P_{n,t} - p_{n+1,t}^d, \forall n \in \Omega_N, t \in \mathcal{T} \quad (11b)$$

$$518 \quad Q_{n+1,t} = Q_{n,t} - q_{n+1,t}^d, \forall n \in \Omega_N, t \in \mathcal{T} \quad (11c)$$

$$519 \quad V_{n+1,t} = V_{n,t} - (b_n^1 P_{n,t} + b_n^2 Q_{n,t}), \forall n \in \Omega_N, t \in \mathcal{T} \quad (11d)$$

$$520 \quad 1 - \varepsilon < V_{n,t} < 1 + \varepsilon, \forall n \in \Omega_N, t \in \mathcal{T} \quad (11e)$$

$$521 \quad 0 \leq p_{i,t}^d \leq \bar{p}_i^d, \forall i \in \mathcal{I}, t \in \mathcal{T} \quad (11f)$$

$$522 \quad 0 \leq q_{i,t}^d \leq \bar{q}_i^d, \forall i \in \mathcal{I}, t \in \mathcal{T} \quad (11g)$$

$$523 \quad 0 \leq P_{n,t} - P_{m,t} \leq \bar{P}_{nm}, \forall (n, m) \in \Omega_L, t \in \mathcal{T} \quad (11h)$$

$$524 \quad 0 \leq Q_{n,t} - Q_{m,t} \leq \bar{Q}_{nm}, \forall (n, m) \in \Omega_L, t \in \mathcal{T} \quad (11i)$$

525 Constraints (11a)–(11i) are the linearized DistFlow equa-  
526 tions, which have been widely applied to calculate the complex

power flow and voltage profile in distribution systems [31]. In  
addition, prices are limited by

$$529 \quad \sum_{t \in \mathcal{T}} c_{i,t}^l = \bar{c}, \forall i \in \mathcal{I} \quad (11j)$$

530 The foregoing utility function (10) and constraints (11a)–(11i)  
531 can be used to formulate the following optimization problem

$$532 \quad \min_{c_{i,t}^l, g_t} -U_D \quad (12a)$$

$$533 \quad s.t. (11a) \quad (12b)$$

534 Moreover, the feasible strategy set of the DMO can be  
535 defined by

$$536 \quad \Omega_D = \left\{ c_{i,t}^l, g_t \mid (11a) \right\}. \quad (13)$$

### 537 C. Stackelberg Equilibrium

538 The desired outcome of the game leads to a Stackelberg  
539 Equilibrium. The formal description of the SE correspond-  
540 ing to the proposed one-leader, non-cooperative n-follower  
541 Stackelberg game can be described as follows [15]. Given the  
542 notation of  $\Omega_C$  and  $\Omega_P$ ,  $(\Omega_C^*, \Omega_P^*)$  is a SE for the proposed  
543 game if it corresponds to the solution of the following bilevel  
544 optimization problem:

$$545 \quad \min_{c_{i,t}^l, p_{i,t}^l, g_t} -U_D \quad (14a)$$

$$546 \quad s.t. c_{i,t}^l, g_t \in \Omega_D \quad (14b)$$

$$547 \quad p_{i,t}^l \in \arg \max_{\tilde{p}_{i,t}^l, \tilde{p}_{i,t}^g} \{U_i : \Omega_i\}, \forall i \in \mathcal{I} \quad (14c)$$

548 Subsequently, we utilize the following theorem to prove  
549 the existence of the SE between the DMO and DRAs in the  
550 proposed game.

*Theorem 1:* For the proposed game, a SE exists if the  
551 following conditions are satisfied [20]:

552 1) The strategy set of each player is nonempty, convex, and  
553 a compact subset of some Euclidean space  $\mathbb{R}$ .

554 2)  $U_D$  is continuous and concave in  $\Omega_C$ .

555 3)  $U_i$  is continuous in  $\mathcal{P}_i$  and concave in  $\mathcal{P}_i, \forall i \in \mathcal{I}$ .

556 *Proof 1):* Because  $\Omega_D$  and  $\Omega_i$  are linear, these sets are read-  
557 ily defined as nonempty, convex, and a compact subset of some  
558 Euclidean space  $\mathbb{R}$ .

559 *Proof 2) and 3):* Because  $\partial^2 U_D / \partial c_{i,t}^l{}^2 = 0$  and  
560  $\partial^2 U_i / \partial p_{i,t}^l{}^2 = 0, \forall i \in \mathcal{I}$ , the SE exists between the leader's  
561 side and followers' side.

562 The uniqueness of the SE is explained in Section V-B, where  
563 the optimal solution of the HDDGD algorithm is a SE.

## 564 V. SOLUTION ALGORITHM

### 565 A. M Penalty Algorithm for the Data-Driven Stage

566 The data-driven problem (4) with the KKT reformulations  
567 can be solved by several off-the-shelf approaches such as  
568 CPLEX non-linear solvers. However, since (4) is NP-hard,  
569 these methods cannot provide a good result for large-scale  
570 applications in a reasonable computational period. Therefore,  
571 this subsection develops a new algorithm to tackle (4), that  
572

is, to solve a linear relaxation of the mathematical program with equilibrium constraints (4) by penalizing violations of the complementarity constraints.

Instead of directly finding the optimal solution to (4), the proposed algorithm leverages historic data to calibrate the solution through the penalty factor  $M$  to minimize out-of-sample prediction errors.

1) *Algorithm Description:* The penalty algorithm utilizes a linear (convex) relaxation of a mathematical programming problem with equilibrium constraints, whereby the complementarity conditions of the lower-level problem in the data-driven stage are transferred to the objective function (4a), penalizing the sum of dual variables in the non-linear constraints of (2) and slacks of (1). In this paper, the slack is defined as the right side minus the left side in the form of a “ $\leq$ ” constraint. For example, the slack of constraint (1b) is:  $r_{i,t}^u - x_{i,t} + x_{i,t-1}$ . This ensures that the slack is always nonnegative.

The penalty method achieves an approximate solution, which helps to provide precisely predicted parameters for the Stackelberg-pricing stage and save computational costs. With the above relaxation of constraints (2d)–(2g), the original objective function (4a) can be recast as:

$$\begin{aligned} \min_{\Omega_R} \sum_{t \in \mathcal{T}} \omega_t (\alpha_{i,t}^+ + \alpha_{i,t}^-) \\ + M \left( \sum_{t \in \mathcal{T}} \omega_t (\bar{\psi}_{i,t} + \underline{\psi}_{i,t} + \bar{P}_{i,t} - \underline{P}_{i,t}) \right. \\ \left. + \sum_{t \in \mathcal{T}_{-1}} \omega_t (\lambda_{i,t}^u + \lambda_{i,t}^d + r_{i,t}^u + r_{i,t}^d) \right) \end{aligned} \quad (15a)$$

where  $\Omega_R = \{x_{i,t}, \theta_{i,t}, \alpha_{i,t}^+, \alpha_{i,t}^-, \bar{\psi}_{i,t}, \underline{\psi}_{i,t}, \lambda_{i,t}^u, \lambda_{i,t}^d\}$  subject to:

$$(4b) - (4c), (1b) - (1d), (2a) - (2c) \quad (15b)$$

$$\lambda_{i,t}^u, \lambda_{i,t}^d \geq 0, t \in \mathcal{T}_{-1} \quad (15c)$$

$$\bar{\psi}_{i,t}, \underline{\psi}_{i,t} \geq 0, t \in \mathcal{T} \quad (15d)$$

The relaxed objective function (15a) includes two items. The first term is the original objective (4a). The second, which includes the sum of dual variables in non-linear complementarity constraints plus their slacks, is multiplied by a penalty coefficient  $M$ . Note that the effect of  $\omega_t$  that multiplies the second and third items is the same as the weights in (3). In addition, the introduction of  $M$  minimizes the out-of-sample prediction error.  $M$  penalizes the sum of dual variables in non-linear constraints of equation set (2) and the slacks of equation set (1). In this way, the relaxed problem (15) is parameterized on  $M$ , which provides our solution approach with a degree of freedom over directly solving (4). Indeed, we can let the data decide which value of  $M$  minimizes the out-of-sample prediction error.

Objective function (15a) is subject to two groups of constraints. The first group includes auxiliary constraints (4b)–(4c). The second group contains the primal and dual feasibility constraints of (1b)–(1d), (2a)–(2c), and (5c)–(5d). Due to the linearity of (15), we can obtain its global

optimum by using linear solvers with a reasonable computational cost.

2) *Statistical Significance of the Developed Algorithm:* It is obvious that the original objective function (4a) only minimizes in-sample prediction errors. In statistical learning theory [32], it is well known that the minimization of in-sample prediction errors is not equivalent to minimizing out-of-sample prediction errors. Accordingly, the estimated DR parameters, i.e., the optimal solution of (4) that aims to minimize in-sample prediction errors, may not be the ones that perform best in future. For example, the in-sample prediction error can be reduced to zero by enlarging the parameter space defining the market bids and overfit the data; however, the out-of-sample prediction error would dramatically increase as a result. As the ultimate goal of the data-driven stage is to minimize out-of-sample errors, the experiment-based penalty algorithm we have developed has a twofold significance compared to solving (4) to optimality. First, it saves computational cost and thus can be applied to both real-time and day-ahead market scenarios. Second, the value of  $M$  can be adjusted by users to minimize the out-of-sample errors. This means that the developed algorithm can provide more accurate predictions and results.

### B. HDDGD Algorithm for Stackelberg-Pricing Stage

Since the proposed  $n$ -follower Stackelberg game has  $n$  parallel lower-level optimization problems and time-variant variables, it is difficult to solve and computationally intensive. Given a fixed pricing strategy  $C_i$ , (5) is a linear programming problem. Similarly, given a fixed consumption strategy  $\mathcal{P}_i$ , (12) is convex. Thus, a Lagrange dual decomposition can be applied to cater the parallel structure and time-series variables of the proposed model, so that the solution can be obtained more easily and in a shorter period of time.

1) *Compact Notation of the Primary Problem:* To demonstrate the proposed HDDGD algorithm, a compact notation is established to denote the Stackelberg-pricing stage. For the follower:

$$\min_{\mathbf{p}_1} \mathbf{c}_1^\top \mathbf{p}_1 + Q(\mathbf{R}) \quad (16a)$$

$$s.t. \mathbf{A}_1 \mathbf{p}_1 \leq \mathbf{b}_1 \quad (16b)$$

$$\mathbf{p}_1 \in \mathcal{P} \quad (16c)$$

where vector  $\mathbf{p}_1 \in \mathbb{R}^{n_1}$  includes decision variables with respect to consumption and controllable DG generation, vector  $\mathbf{c}_1^\top \in \mathbb{R}^{n_1}$  represents electricity prices,  $\mathbf{R} \in \mathbb{R}^{d_1}$  represents the constants in (7),  $\mathbf{b}_1 \in \mathbb{R}^{m_1}$  and  $\mathbf{A}_1 \in \mathbb{R}^{m_1 \times n_1}$  denote load ramp constraints (5b)–(5c), and  $\mathcal{P}$  indicates consumption limits (5d)–(5i). For the leader:

$$\min_{\mathbf{p}_2, \mathbf{c}_2, \mathbf{g}} \mathbf{p}_2^\top \mathbf{c}_2 + f(\mathbf{g}) \quad (17a)$$

$$s.t. \mathbf{A}_2(\mathbf{g}, \mathbf{c}_2)^\top = \mathbf{b}_2 \quad (17b)$$

where vector  $\mathbf{p}_2^\top \in \mathbb{R}^{n_2}$  denotes the consumptions of the DRAs,  $\mathbf{c}_2 \in \mathbb{R}^{n_1 \times n}$  represents the pricing strategies for all DRAs,  $\mathbf{g} \in \mathbb{R}^{d_2}$  is the purchased electricity in all related expressions  $f(\mathbf{g})$ , and  $\mathbf{A}_2 \in \mathbb{R}^{m_2 \times (d_2 + n_1 \times n)}$  and  $\mathbf{b}_2 \in \mathbb{R}^{m_2}$  denote operational security and price constraints (11a)–(11j).

675 2) *Dual Decomposition and Gradient Descent Method:*  
 676 For the follower, according to the compact notation, the  
 677 Lagrangian is:

$$678 \quad L(\mathbf{u}_1, \mathbf{p}_1) = \mathbf{c}_1^\top \mathbf{p}_1 + \mathcal{Q}(\mathbf{R}) - \mathbf{u}_1^\top (\mathbf{A}_1 \mathbf{p}_1 - \mathbf{b}_1) \quad (18)$$

679 with a vector of nonnegative Lagrange multipliers  $\mathbf{u}_1 \in \mathbb{R}^{n_1}$ .  
 680 The dual objective is

$$681 \quad L(\mathbf{u}_1) = \min_{\mathbf{p}_1 \in \mathcal{P}} L(\mathbf{u}_1, \mathbf{p}_1) \quad (19)$$

682 and the dual problem is to find

$$683 \quad \max_{\mathbf{u}_1 \in \mathbb{R}^{n_1}} L(\mathbf{u}_1) \quad (20)$$

684 Let  $p_k$  and  $c_k$  be an element of  $\mathbf{p}_1$  and  $\mathbf{c}_1$ , respectively, let  $\mathbf{A}_k$   
 685 be the coefficient vector of  $p_k$  in  $\mathbf{A}_1$ , let  $\mathbf{u}_k$  be the Lagrange  
 686 multiplier vector of  $p_k$ ,  $k = 2n + 1, n \in \mathbb{Z}$ , and let  $(\kappa)_{k=1}^K$   
 687 denote the operation of concatenating all elements  $\kappa_1, \dots, \kappa_K$   
 688 into a single column vector. Then, (18) with respect to  $p_k$  can  
 689 be rewritten as

$$690 \quad \min_{p_k \in \mathcal{P}} L(\mathbf{u}_1, p_k) \\ 691 \quad = (c_k p_k)_{k=1}^{n_1-1} + \mathcal{Q}(\mathbf{R}) - \mathbf{u}_1^\top (\mathbf{A}_1 (\mathbf{p}_k)_{k=1}^{n_1-1} - \mathbf{b}_1) \quad (21)$$

692 To facilitate the calculation of time-dependent  $p_k$  in the cou-  
 693 pling constraint (16b), we apply a sub-gradient algorithm to  
 694 the dual decomposition [33]:

$$695 \quad (p_k^{(q)})_{k=1}^{n_1-1} = \arg \min_{p_k \in \mathcal{P}} L(\mathbf{u}_1^{(q-1)}, p_k) = \left( \arg \min_{p_k \in \mathcal{P}} c'_k p_k \right)_{k=1}^{n_1-1} \quad (22a)$$

$$697 \quad \mathbf{u}_1^{(q)} = \mathbf{u}_1^{(q-1)} + \delta_1 \left( \mathbf{A}_1 (p_k^{(q)})_{k=1}^{n_1-1} - \mathbf{b}_1 \right) \quad (22b)$$

698 where  $\delta_1 > 0$  is a step size and  $c'_k = c_k + \mathbf{A}_k^\top \mathbf{u}_k$ . Thus the  
 699 dual problem decomposes into  $n_1/2$  maximization problems  
 700 that can be easily solved with zero duality gap.

701 The leader offers an optimal price vector  $\mathbf{c}_2^*$  given the  
 702 best response  $\mathbf{p}_2^*$ . With a vector of nonnegative Lagrange  
 703 multipliers  $\mathbf{u}_2 \in \mathbb{R}^{(d_2+n_1 \times n)}$ , the Lagrangian dual objective is:

$$704 \quad \min_{\mathbf{c}_2, \mathbf{g}} L(\mathbf{u}_2, \mathbf{c}_2, \mathbf{p}_2^*) = \mathbf{p}_2^{*\top} \mathbf{c}_2 + f(\mathbf{g}) - \mathbf{u}_2^\top (\mathbf{A}_2(\mathbf{g}, \mathbf{c}_2)^\top - \mathbf{b}_2) \quad (23)$$

706 Similar to (22), we have:

$$707 \quad (\mathbf{c}_2^{(q)}, \mathbf{g}^{(q)}) = \arg \min_{\mathbf{c}_2, \mathbf{g}} L(\mathbf{u}_2^{(q-1)}, \mathbf{c}_2, \mathbf{p}_2^*) \quad (24a)$$

$$708 \quad \mathbf{u}_2^{(q)} = \mathbf{u}_2^{(q-1)} + \delta_2 \left( \mathbf{A}_2(\mathbf{g}^{(q)}, \mathbf{c}_2^{(q)})^\top - \mathbf{b}_2 \right) \quad (24b)$$

709 If there exists a solution (no matter whether it is locally  
 710 optimal), the global optimal solution can be obtained by  
 711 applying the above gradient descent method [34]. From  
 712 Sections IV-C and V-B2, we know that each player obtains the  
 713 unique SE after the proposed distributed algorithm is applied.  
 714 This unique SE also represents the global optimality of the  
 715 problem.

---

### Algorithm 1: Distributed HDDGD Algorithm Combined With Penalty Algorithm

---

**Input:**  $q \leftarrow 0, x_{i,t}^h, M, \text{initial}, \epsilon, \theta_{i,t}, \mathcal{C}_i^{(q)}, \mathcal{P}_i^{(q)}, |\mathcal{P}_i^{(q+1)} - \mathcal{P}_i^{(q)}| > \epsilon,$   
 $\mathbf{u}_1^{(q)}, \delta_1, \mathbf{u}_2^{(q)}, \delta_2;$   
**Output:**  $\Omega_C$  and  $\Omega_P;$

```

1 for  $i \in \mathcal{I}$  do
2   Train data according to (15);
3   Deliver estimated  $\theta_{i,t}$  to (5) according to (6);
4 end
5 while  $|\mathcal{P}_i^{(q+1)} - \mathcal{P}_i^{(q)}| > \epsilon$  do
6   for  $i \in \mathcal{I}$  do
7     for  $t \in \mathcal{T}, t \leftarrow 2n + 1, n \leftarrow 0, n + +$  do
8       Given  $\mathcal{C}_i^{(q)}$ , DRA  $i$  calculate  $p_{i,t}^{(q+1)}$  according to (22a);
9       Update the dual variable by using (22b):
10       $u_{i,t}^{1(q+1)} \leftarrow (u_{i,t}^{1(q)} + \delta_1^1 (p_{i,t}^{(q+1)} - p_{i,t}^{(q)} - r_{i,t}^u))^+;$ 
11       $u_{i,t}^{2(q+1)} \leftarrow (u_{i,t}^{2(q)} + \delta_1^2 (p_{i,t}^{(q+1)} - p_{i,t}^{(q)} - r_{i,t}^d))^+;$  where
12       $\delta_1 > 0$  is sufficiently small;
13    end
14  end
15  Given  $\mathcal{P}_i^{(q+1)}, i \in \mathcal{I}$ , the DMO updates  $\Omega_C^{(q+1)}$  according to (24a);
16  Deliver  $\Omega_C^{(q+1)}$  to DRAs;
17  Update the dual variable by using (24b), where  $\delta_2 > 0$  is
18  sufficiently small;
19 end
20 return Output;
```

---

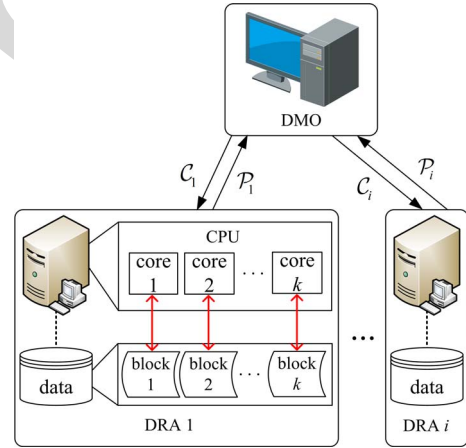


Fig. 2. Detailed operation and implementation of Algorithm 1, where the red arrows represent steps 2–3 and 7–10, and the black arrows correspond to steps 12–13.

716 3) *Combined Distributed Algorithm:* Pseudo code of the  
 717 combined algorithm for the two-stage framework is shown in  
 718 **Algorithm 1**, where step numbers are shown on the left side.

719 The proposed algorithm can be implemented in parallel.  
 720 Fig. 2 shows the detailed operation and implementation of  
 721 **Algorithm 1** in a market management system.

722 In a DRA, the server applies multi-string processing to  
 723 steps 2–3 in the data-driven stage to speed up calculation.  
 724 In the Stackelberg-pricing stage, single-program multiple-data  
 725 (SPMD)-based parallel computing can be used since (16)  
 726 can be decomposed into multiple independent subproblems  
 727 through step 9 [35]. The workload of (16) is distributed to  
 728 different cores of the CPU. The parameters of the decom-  
 729 posed problems, such as  $c'_k$  and  $\mathcal{P}$ , are stored in different data  
 730 blocks, where the cores run different decomposed problems in  
 731 parallel.

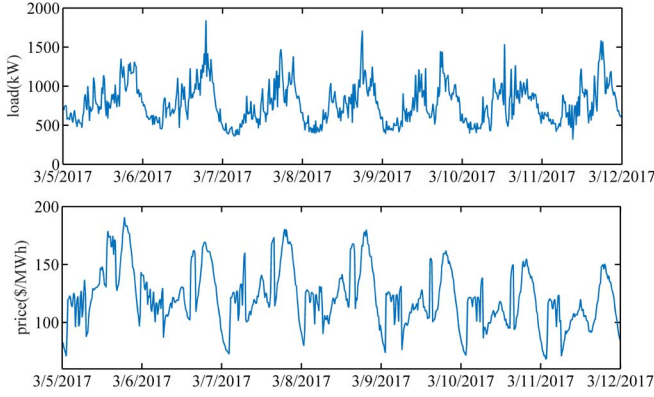


Fig. 3. A sample dataset from the 2-month training set.


 Fig. 4. (a) Three DRA-managed regions, enclosed within the black lines, in Shandong, China, and (b) MAPEs with respect to different values of  $M$  and  $F$ .

732 In the DMO, the price strategy  $\Omega_C$  can only be calculated  
 733 using  $\Omega_P$  through step 12 since the market rule does not allow  
 734 the DMO to access the full information of DRAs, followed by  
 735 the DMO revealing  $\Omega_P$  to the DRAs. Each DRA can calculate  
 736 its  $\mathcal{P}_i$  given the revealed  $\mathcal{C}_i$  through steps 8–9. The process  
 737 repeats until the game converges to a unique SE.

## VI. CASE STUDIES

738  
 739 The proposed method was tested on a realistic DR project  
 740 in China using the IEEE 33-bus test feeder that included 4  
 741 DRAs and a larger distribution system. All calculations were  
 742 performed on the Iowa State University Condo cluster with  
 743 two 2.6 GHz 8-core Intel E5v3 processors, 128 GB RAM,  
 744 and CPLEX 12.6 under GAMS.

### A. Data-Mining Methods

746 To test the predictive accuracy of the proposed data-driven  
 747 method, experiments were implemented on the Changdao  
 748 project in Shandong China, where 15-minute day-ahead elec-  
 749 tricity prices were sent to three similar DRAs, each with  
 750 157 households, through the proposed pricing strategy. Each  
 751 DRA's households then consumed electricity based on the  
 752 given prices on the next day. The price-sensitive smart con-  
 753 trollers installed in each house controlled appliances and  
 754 plug-in electric vehicles (PEV) based on the house owner's  
 755 preferences. Appliances in the home included controllable  
 756 (space cooling/heating, water heating, and clothes washing)  
 757 and critical (cooking, lighting, refrigerator, freezer, and oth-  
 758 ers) systems. The total penetration of the PEVs was 13.2%.  
 759 Fig. 3 depicts a sample training dataset of a DRA's practi-  
 760 cal price-load data. Fig. 4(a) identifies the 3 DRA-managed  
 761 regions on a geographical map. To validate the performance  
 762 of the proposed data-driven method, the following cases  
 763 were compared: 1) ARX [32] DR modeling; 2) the proposed  
 764 inverse optimization-based DR modeling solved by an off-  
 765 the-shelf CPLEX solver (InvC); and 3) the proposed inverse  
 766 optimization-based modeling with the newly developed  $M$ -  
 767 penalty algorithm (Inv). Note that all of the above cases used  
 768 the same pricing strategy as proposed in Section IV.

769 Before the tests, we first determined the values of the  
 770 parameters  $M$  and  $F$  for the proposed load modeling method.

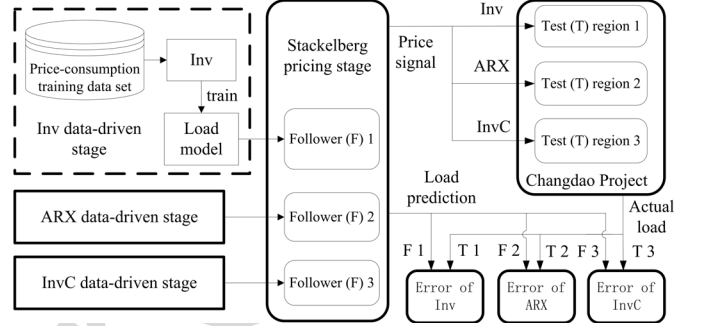


Fig. 5. Flow chart to test the data-driven method.

A combination of these parameters were searched to mini-  
 771 mize validation errors. We utilized cross-validation to perform  
 772 a sensitivity analysis of  $M$  and  $F$  by mean absolute percentage  
 773 error (MAPE). Fig. 4(b) illustrates this MAPE with respect to  
 774 different combinations of  $M$  and  $F$ . From the figure, we can  
 775 see that  $M = 0.2$  and  $F = 1$  result in the best prediction  
 776 performance that minimizes out-of-sample errors.

777  
 778 As illustrated in Fig. 5, the test was conducted in three  
 779 steps. First, the above 3 cases were simultaneously imple-  
 780 mented on 3 DRAs as the data-driven stage of the market  
 781 strategy, where each case produced a set of day-ahead prices  
 782 and consumption predictions. Second, each DRA's households  
 783 resulted in a set of actual consumptions on the next day.  
 784 Finally, each case's prediction performance was calculated  
 785 by comparing the predicted and actual consumption of the  
 786 corresponding DRA.

787 Results from two consecutive days over the March 24 to 27,  
 788 2017 period are shown in Fig. 6. The ARX method provides  
 789 good performance, but can not follow sudden load changes.  
 790 The InvC method has an overfitting problem. Biased prices  
 791 were decided under this overfitting, leading to a worse DR  
 792 performance. The Inv method has the best performance with  
 793 reasonable out-of-sample errors. In addition, we used four met-  
 794 rics to measure the prediction performance in March in Table I:  
 795 MAPE, root mean square error (RMSE), mean absolute error  
 796 (MAE), and computational time (CT). In terms of prediction-  
 797 error minimization, the Inv method is better than ARX and  
 798 InvC. Although Inv takes more calculation time than ARX  
 799 due to higher dimensions in the explanatory variable vector, it  
 800 is still acceptable for day-ahead markets.

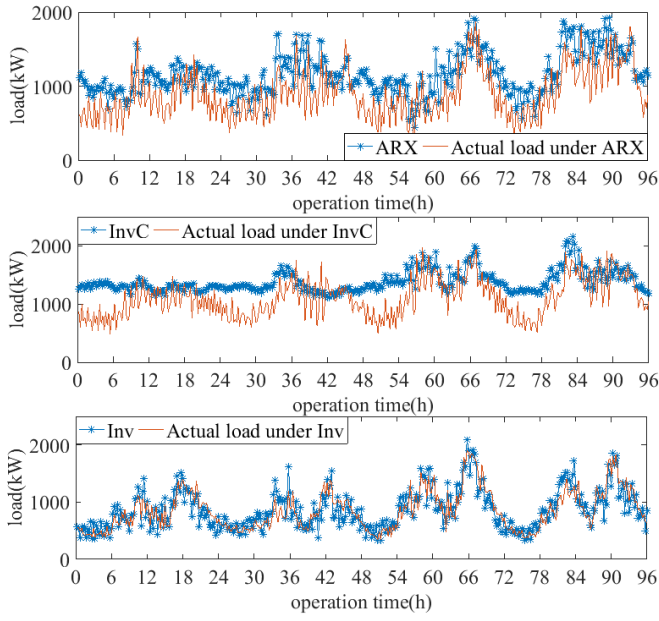


Fig. 6. Actual and forecasted load during 24-27 Mar., 2017.

TABLE I  
PERFORMANCE OF DIFFERENT DATA-DRIVEN METHODS IN MARCH

	MAPE	RMSE	MAE	CT(s)
ARX	19.178	23.421	0.1869	503
InvC	57.639	69.473	0.6371	3076
Inv	12.102	15.602	0.0963	897

TABLE II  
DG AND CONSUMER DATA OF DRAS

DRA	Micro-Turbine (MT)			PV Generator		Number of Users	Node in IEEE 33-Bus
	Output Limit (kW)	Ramp Up/Down Rate (kW/h)	Operation Cost (\$/kWh)	Nominal Rating (kW)	Normalized Standard Deviation		
1	500	430/470	0.15	1250	5.1%	127	24
2	375	280/300	0.2	650	5.3%	98	31
3	375	280/300	0.2	1300	5.0%	109	15
4	300	200/230	0.25	375	5.1%	75	21

### B. Pricing Strategies

Numerical simulations were performed on an IEEE 33-bus distribution system [31] with 4 connected DRAs. Each DRA had different groups of end users, whose training data sets were pulled from the Changdao project database. For example, data for 127 users was randomly selected from this database to form an aggregated training set for DRA 1. Table II presents the setups for the DRAs obtained from the Changdao project, which were mapped to the IEEE 33-bus system. The simulation parameters were set as follows: penalty factor  $\gamma_t = \$9.00/\text{kWh}$  [36];  $\varepsilon = 0.02$  p.u.;  $\mu = \$0.17/\text{kWh}$ ;  $M = 0.2$ ;  $\bar{c} = \$3.60/\text{kWh}$ ;  $\omega_t$  was obtained from historical real-time market prices;  $c_t$  and  $\bar{g}_t$  can be found in [24]. For **Algorithm 1**:  $\epsilon = 0.01$ ;  $\delta_1 = [0.05, 0.05]$ ,  $\delta_2 = 0.03$ ; and  $T = 24h$ .

1) *Load Peak Shaving*: The two benchmarks used for comparing the results from the proposed method in this work were flat rate (FR) and time-of-use (TOU) pricing schemes. For illustrative purposes, the mean and standard deviation of the consumptions of the four DRAs are depicted in Fig. 7. Under

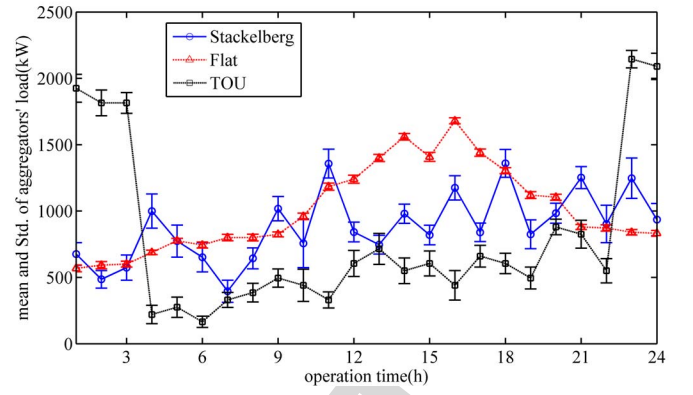


Fig. 7. Mean and standard deviation of four DRAs on 13 Feb., 2017.

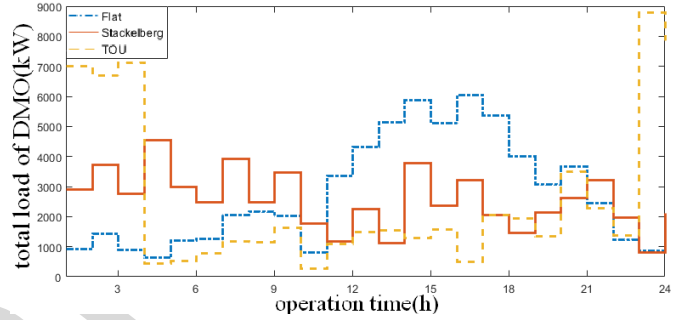


Fig. 8. Load profiles of the distribution system.

TABLE III  
ECONOMIC PERFORMANCE OF BENCHMARKS

Benchmark	Market Type	Follower Level Costs (\$)	DMO Costs (\$)	Total Costs (\$)	CT (s)
TOU	Day-ahead	2994.4	-1215.9	1778.5	842
	Real-time	1137.6	-142.9	994.7	24
PS	Day-ahead	2867.3	-1596.4	1270.9	973
	Real-time	569.6	-200.1	369.5	16

the FR strategy, each aggregator's end users had no incentive to minimize their power usage and resulting costs. Although TOU shaves the original peak between 10:00-21:00 by a lower price, undesirable load pickup occurs between 22:00-4:00 with a large standard deviation. Note that the FR and TOU strategies are predefined, and cannot represent the interactions between DRAs and the DMO. Under the proposed strategy, the overall load profile was smoothed, since the pricing scheme was dynamic. When a lower price promoted a DRA to consume more power, the DMO raised the price to make more profit, leading to a lower consumption.

In Fig. 8, the proposed pricing strategy shaves the total peak load of the distribution system. When some DRAs consume more power, the DMO raises the prices of these DRAs to make more profit, leading to their lower consumption.

2) *Operational Security*: We compare our method to the game model proposed in [19], which does not consider operational constraints. Fig. 9 shows 24 h mean voltage values at representative nodes. We can see that the model in [19] may lead to voltage violations.

3) *Economic Performance*: We compare the economic performances of the proposed Stackelberg strategy and the TOU, with results shown in Table III.

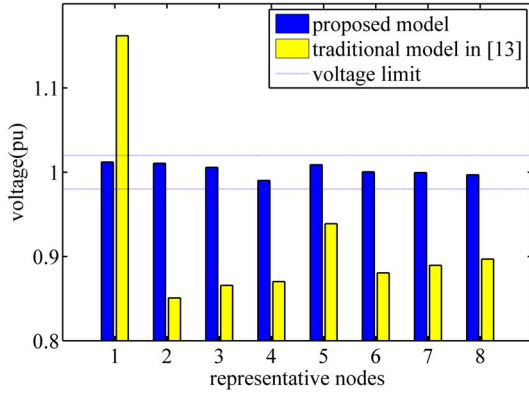


Fig. 9. Voltage profiles under two game models.

TABLE IV  
INFORMATION OF DRAS

DRA	MT Total Max Output (kW)	Renewable Penetration Level (%)	Type
1	650	8.6	Residential
2		14.7	
3		19.3	
4	300	0	Commercial
5	750	2.6	
6	1050	0	

In Table III, PS outperforms TOU in several economic aspects such as DAR costs, DMO costs, and total costs under the same conditions. Since end users in the day-ahead market are well satisfied through DR management of PS, total costs of the real-time market are less than with TOU pricing. In addition, the proposed game model for day-ahead and real-time markets converges at the SE with iteration numbers of 17 and 8, respectively.

C. Test on a Larger System

The proposed strategy was then applied to a real distribution system in the Changdao project with 128 nodes and 7 DRAs. Due to data confidentiality, only details important to understand the results are provided. The single line diagram of the system is shown in Fig. 10. Table IV lists the DRA information. The appliance types are the same as described in the system in Fig. 4, and the total penetration of EVs was 11.3%.

- The following test cases (TC) were considered:
- TC 1: the distribution system included DRA 1 and DRA 4
- TC 2: the distribution system included DRA 2 and DRA 4
- TC 3: the distribution system included DRA 3 and DRA 4
- TC 4: the distribution system included DRA 1-6

Information pertaining to the local renewable energy generators, load outputs, and training data set can be found in the historical data of the project. The remaining parameters were derived from the project and the previous case study conducted in this paper.

To analyze the impact of renewable integration, the results from the simulations for TC 1-4 are found in Table V and Fig. 11.

TABLE V  
SIMULATION PERFORMANCE UNDER DIFFERENT PENETRATION LEVELS

TC	TOU		PS	
	Operation Costs (\$)	CT (s)	Operation Costs (\$)	CT (s)
1	3498.4	682	3017.6	703
2	3649.2	720	3111.9	729
3	3834.6	739	3195.5	737

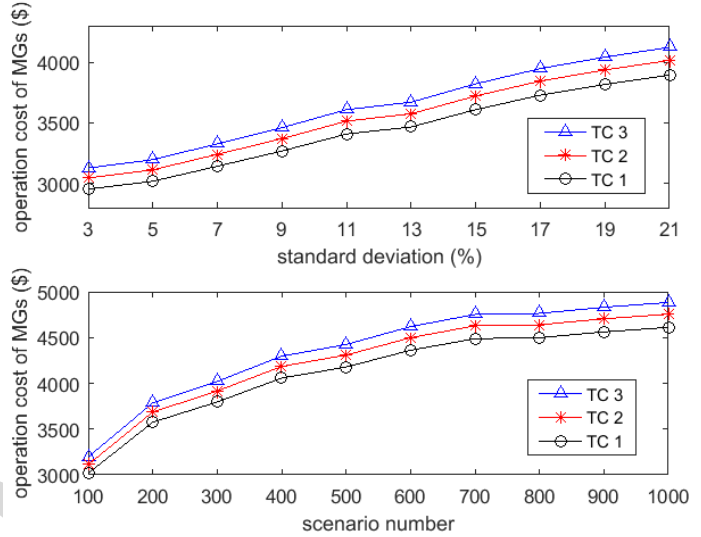


Fig. 11. PS sensitivity analysis: (a) operational costs versus standard deviation of renewable generation forecasting error, and (b) operational costs versus number of scenarios.

TABLE VI  
SIMULATION RESULTS OF PS IN TC 4 OVER 60 SIMULATION RUNS

Market Scenario	Optimal Solution of Operation Costs (\$)			Average Iteration Number	Average CT (s)
	Minimum (Best)	Average	Maximum (Worst)		
Day-ahead	15943.721	15943.721	15943.72	18	994
Real-time	2862.686	2862.685	2862.685	8	21

In Table V, PS outperforms TOU under different renewable penetration levels, since PS considers the uncertainty of renewables and the dynamic pricing. The operational costs increase as the renewable penetration level increases from TC 1 to TC 3, since more costs are taken to mitigate the fluctuation introduced by the higher renewable penetration. From TC 1 to TC 2, there is a 3.1% increase in PS operational costs caused by a 4.1% increase in renewable integration, while the TOU operational cost percentage increase is 4.3%. From TC 2 to TC 3, a 2.7% increase in PS operational costs is caused by a 3.2% increased renewable integration, while the TOU operational costs increase by 5.1%.

Fig. 11(a) shows that a higher variance in renewable generation leads to a higher operational cost. Fig. 11(b) demonstrates that the operational costs converge as the number of scenarios increases.

To illustrate the effectiveness of the PS method, 60 independent simulations were performed in TC 4, with the results shown in Table VI.

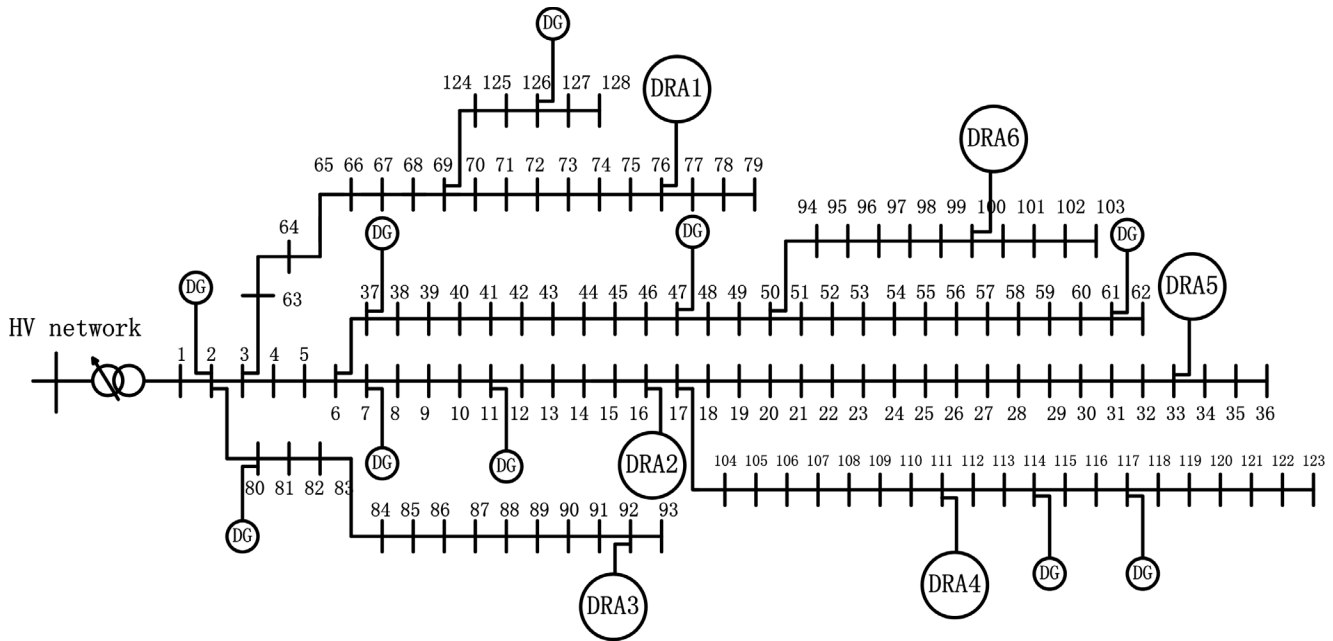


Fig. 10. Single line diagram of the real system.

893 It can be seen that in a large system with 6 different DRAs,  
894 PS can still converge in a reasonable time.

## 895 VII. CONCLUSION

896 This paper proposed a data-driven Stackelberg market strategy  
897 for DR-enabled distribution systems, which coordinates  
898 multiple profit-pursuing entities (DRAs or VPPs) and bridges  
899 the regulation gap between the ISO and distribution systems.  
900 For the data-driven stage, an innovative inverse method was  
901 developed to train the DR model, which achieves good  
902 prediction performance and presents a generalized computationally  
903 light modeling approach. Considering operational  
904 practice in retail markets, a Stackelberg game-based pricing  
905 strategy was designed to maximize each market participant's  
906 profit and guarantee operational security. An efficient M-penalty  
907 algorithm was developed for the data-driven stage  
908 to minimize out-of-sample errors and save computational  
909 cost. A distributed HDDGD algorithm was proposed for the  
910 Stackelberg-pricing stage to obtain an n-follower time-series-  
911 based SE within a reasonable calculation period.

912 Through real-life experiment-based comparisons with two  
913 groups of benchmarks, i.e., data-driven models and pricing  
914 strategies, and simulations on different distribution systems,  
915 we found that our data-driven load modeling method can real-  
916 ize fast computation and accurate prediction, and that our  
917 pricing strategy can achieve peak load shaving, operational  
918 security, and economic profits.

## 919 REFERENCES

920 [1] Y. W. Law, T. Alpcan, and M. Palaniswami, "Security games for risk  
921 minimization in automatic generation control," *IEEE Trans. Power Syst.*,  
922 vol. 30, no. 1, pp. 223–232, Jan. 2015.  
923 [2] T. Lu, Z. Wang, Q. Ai, and W.-J. Lee, "Interactive model for energy  
924 management of clustered microgrids," *IEEE Trans. Ind. Appl.*, vol. 53,  
925 no. 3, pp. 1739–1750, May/June 2017.

[3] A. Zakariazadeh, S. Jadid, and P. Siano, "Smart microgrid energy and  
926 reserve scheduling with demand response using stochastic optimization,"  
927 *Int. J. Elect. Power Energy Syst.*, vol. 63, pp. 523–533, Dec. 2014.  
928 [4] Z. Wang and Y. He, "Two-stage optimal demand response with battery  
929 energy storage systems," *IET Gener. Transm. Distrib.*, vol. 10, no. 5,  
930 pp. 1286–1293, Apr. 2016.  
931 [5] C. Li, X. Yu, W. Yu, G. Chen, and J. Wang, "Efficient computation for  
932 sparse load shifting in demand side management," *IEEE Trans. Smart  
933 Grid*, vol. 8, no. 1, pp. 250–261, Jan. 2017.  
934 [6] L. Gkatzikis, I. Koutsopoulos, and T. Salonidis, "The role of aggregators  
935 in smart grid demand response markets," *IEEE J. Sel. Areas Commun.*,  
936 vol. 31, no. 7, pp. 1247–1257, Jul. 2013.  
937 [7] C. Vivekananthan, Y. Mishra, G. Ledwich, and F. Li, "Demand response  
938 for residential appliances via customer reward scheme," *IEEE Trans.  
939 Smart Grid*, vol. 5, no. 2, pp. 809–820, Mar. 2014.  
940 [8] G. Liu, Y. Xu, and K. Tomovic, "Bidding strategy for microgrid in  
941 day-ahead market based on hybrid stochastic/robust optimization," *IEEE  
942 Trans. Smart Grid*, vol. 7, no. 1, pp. 227–237, Jan. 2016.  
943 [9] S. Shao, M. Pipattanasomporn, and S. Rahman, "Development of  
944 physical-based demand response-enabled residential load models," *IEEE  
945 Trans. Power Syst.*, vol. 28, no. 2, pp. 607–614, May 2013.  
946 [10] T. X. Nghiem and C. N. Jones, "Data-driven demand response modeling  
947 and control of buildings with Gaussian processes," in *Proc. Amer.  
948 Control Conf. (ACC)*, Seattle, WA, USA, May 2017, pp. 2919–2924.  
949 [11] S. Shenoy and D. Gorinevsky, "Data-driven stochastic pricing and applica-  
950 tion to electricity market," *IEEE J. Sel. Topics Signal Process.*, vol. 10,  
951 no. 6, pp. 1029–1039, Sep. 2016.  
952 [12] L. Wang, Z. Zhang, and J. Chen, "Short-term electricity price forecasting  
953 with stacked denoising autoencoders," *IEEE Trans. Power Syst.*, vol. 32,  
954 no. 4, pp. 2673–2681, Jul. 2017.  
955 [13] P. Yang, G. Tang, and A. Nehorai, "A game-theoretic approach for  
956 optimal time-of-use electricity pricing," *IEEE Trans. Power Syst.*,  
957 vol. 28, no. 2, pp. 884–892, May 2013.  
958 [14] Q. Cui, X. Wang, X. Wang, and Y. Zhang, "Residential appliances direct  
959 load control in real-time using cooperative game," *IEEE Trans. Power  
960 Syst.*, vol. 31, no. 1, pp. 226–233, Jan. 2016.  
961 [15] M. Yu and S. H. Hong, "A real-time demand-response algorithm for  
962 smart grids: A Stackelberg game approach," *IEEE Trans. Smart Grid*,  
963 vol. 7, no. 2, pp. 879–888, Mar. 2016.  
964 [16] G. E. Rahi, S. R. Etesami, W. Saad, N. Mandayam, and H. V. Poor,  
965 "Managing price uncertainty in prosumer-centric energy trading: A  
966 prospect-theoretic Stackelberg game approach," *IEEE Trans. Smart Grid*,  
967 to be published.  
968 [17] G. S. Aujla, M. Singh, N. Kumar, and A. Zomaya, "Stackelberg game  
969 for energy-aware resource allocation to sustain data centers using RES,"  
970 *IEEE Trans. Cloud Comput.*, to be published.  
971

AQ4

AQ5

972 [18] M. Latifi, A. Khalili, A. Rastegarnia, and S. Sanei, "Fully distributed  
973 demand response using the adaptive diffusion-Stackelberg algorithm,"  
974 *IEEE Trans. Ind. Informat.*, vol. 13, no. 5, pp. 2291-2301, Oct. 2017.

975 [19] M. Jenabi, S. M. T. F. Ghomi, and Y. Smeers, "Bi-level game approaches  
976 for coordination of generation and transmission expansion planning  
977 within a market environment," *IEEE Trans. Power Syst.*, vol. 28, no. 3,  
978 pp. 2639-2650, Aug. 2013.

979 [20] L. Ma, N. Liu, J. Zhang, W. Tushar, and C. Yuen, "Energy management  
980 for joint operation of CHP and PV prosumers inside a grid-connected  
981 microgrid: A game theoretic approach," *IEEE Trans. Ind. Informat.*,  
982 vol. 12, no. 5, pp. 1930-1942, Oct. 2016.

983 [21] M. V. Afonso, J. M. Bioucas-Dias, and M. A. T. Figueiredo, "An aug-  
984 mented Lagrangian approach to the constrained optimization formulation  
985 of imaging inverse problems," *IEEE Trans. Image Process.*, vol. 20,  
986 no. 3, pp. 681-695, Mar. 2011.

987 [22] G. Marjanovic and V. Solo, "On  $l_q$  optimization and sparse inverse  
988 covariance selection," *IEEE Trans. Signal Process.*, vol. 62, no. 7,  
989 pp. 1644-1654, Apr. 2014.

990 [23] R. K. Ahuja and J. B. Orlin, "Inverse optimization," *Oper. Res.*, vol. 49,  
991 no. 5, pp. 771-783, 2001.

992 [24] N. H. Tran *et al.*, "How geo-distributed data centers do demand response:  
993 A game-theoretic approach," *IEEE Trans. Smart Grid*, vol. 7, no. 2,  
994 pp. 937-947, Mar. 2016.

995 [25] S. Parhizi, A. Khodaei, and M. Shahidehpour, "Market-based vs. price-  
996 based microgrid optimal scheduling," *IEEE Trans. Smart Grid*, to be  
997 published.

998 [26] A. Aswani, Z.-J. M. Shen, and A. Siddiq, "Inverse optimization with  
999 noisy data," *arXiv preprint arXiv:1507.03266*, 2015.

1000 [27] J. Saez-Gallego, J. M. Morales, M. Zugno, and H. Madsen, "A data-  
1001 driven bidding model for a cluster of price-responsive consumers of  
1002 electricity," *IEEE Trans. Power Syst.*, vol. 31, no. 6, pp. 5001-5011,  
1003 Nov. 2016.

1004 [28] T. Başar and G. J. Olsder, *Dynamic Noncooperative Game Theory*.  
1005 Philadelphia, PA, USA: SIAM, 1998.

1006 [29] Z. Ding and W.-J. Lee, "A stochastic microgrid operation scheme to  
1007 balance between system reliability and greenhouse gas emission," *IEEE*  
1008 *Trans. Ind. Appl.*, vol. 52, no. 2, pp. 1157-1166, Mar./Apr. 2016.

1009 [30] C. Valente, G. Mitra, M. Sadki, and R. Fourer, "Extending alge-  
1010 braic modelling languages for stochastic programming," *INFORMS J.*  
1011 *Comput.*, vol. 21, no. 1, pp. 107-122, 2009.

1012 [31] M. E. Baran and F. F. Wu, "Network reconfiguration in distribution  
1013 systems for loss reduction and load balancing," *IEEE Trans. Power Del.*,  
1014 vol. 4, no. 2, pp. 1401-1407, Apr. 1989.

1015 [32] J. Friedman, T. Hastie, and R. Tibshirani, *The Elements of Statistical*  
1016 *Learning* (Springer Series in Statistics), vol. 1. Berlin, Germany:  
1017 Springer, 2001.

1018 [33] A. M. Rush and M. Collins, "A tutorial on dual decomposition and  
1019 Lagrangian relaxation for inference in natural language processing," *J.*  
1020 *Artif. Intell. Res.*, vol. 45, no. 1, pp. 305-362, 2012.

1021 [34] D. P. Bertsekas, *Nonlinear Programming*. Belmont, MA, USA: Athena  
1022 Sci., 1999.

1023 [35] W.-C. Kao, J.-C. Tsai, and Y.-C. Chiu, "Parallel computing architecture  
1024 for eye tracking systems," in *Proc. IEEE Int. Conf. Consum. Electron.*  
1025 *Taiwan (ICCE TW)*, Taipei, Taiwan, Jun. 2017, pp. 289-290.

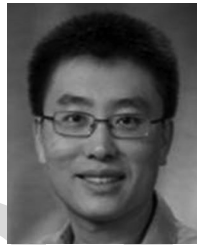
1026 [36] K. K. Kariuki and R. N. Allan, "Evaluation of reliability worth and  
1027 value of lost load," *IEE Proc. Gener. Transm. Distrib.*, vol. 143, no. 2,  
1028 pp. 171-180, Mar. 1996.



**Zhaoyu Wang** (S'13-M'15) received the B.S. and M.S. degrees in electrical engineering from Shanghai Jiaotong University in 2009 and 2012, respectively, and the M.S. and Ph.D. degrees in electrical and computer engineering from the Georgia Institute of Technology in 2012 and 2015, respectively. He is the Harpole-Pentair Assistant Professor with Iowa State University.

He was a Research Aid with Argonne National Laboratory in 2013, and an Electrical Engineer with Corning Inc. in 2014. His research interests include power distribution systems, microgrids, renewable integration, power system resiliency, demand response, and voltage/VAR control.

Dr. Wang was a recipient of the IEEE PES General Meeting Best Paper Award in 2017 and the IEEE Industrial Application Society Prize Paper Award in 2016. He serves as the Secretary of IEEE PES Awards Subcommittee. He is an Editor of the IEEE TRANSACTIONS ON SMART GRID and the IEEE POWER ENGINEERING LETTERS. His research projects are currently funded by the U.S. National Science Foundation, the U.S. Department of Energy, National Laboratories, PSERC, and Iowa Economic Development Agency and Industry.



**Jianhui Wang** (S'07-M'12) received the Ph.D. degree in electrical engineering from the Illinois Institute of Technology, Chicago, IL, USA, in 2007.

He is currently an Associate Professor with the Department of Electrical Engineering, Southern Methodist University, Dallas, TX, USA. He also holds a joint appointment as a Section Lead for Advanced Power Grid Modeling with the Energy Systems Division, Argonne National Laboratory, Argonne, IL, USA.

Dr. Wang was a recipient of the IEEE Power and Energy Society (PES) Power System Operation Committee Prize Paper Award in 2015. He is the Secretary of the IEEE PES Power System Operations, Planning and Economics Committee. He is an Associate Editor of the *Journal of Energy Engineering* and an Editorial Board Member of *Applied Energy*. He has held visiting positions in Europe, Australia, and Hong Kong, including a VELUX Visiting Professorship with the Technical University of Denmark. He is the Editor-in-Chief of the IEEE TRANSACTIONS ON SMART GRID and an IEEE PES Distinguished Lecturer.

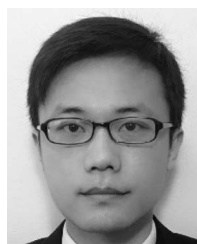


**Qian Ai** (S'03-M'16) received the bachelor's degree in electrical engineering from Shanghai Jiao Tong University, Shanghai, China, in 1991, the master's degree in electrical engineering from Wuhan University, Wuhan, China, in 1994, and the Ph.D. degree in electrical engineering from Tsinghua University, Beijing, China, in 1999.

He was with Nanyang Technological University, Singapore, for one year, the University of Bath, Bath, U.K., for two years, and then with Shanghai Jiao Tong University, where he is currently a Professor

with the School of Electronic Information and Electrical Engineering. His current research interests include power quality, load modeling, smart grids, microgrid, and intelligent algorithms.

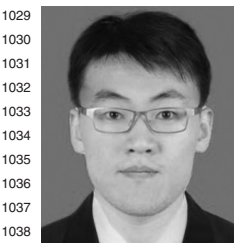
Prof. Ai was a recipient of the IEEE Industrial Application Society Prize Paper Award in 2016.



**Chong Wang** (M'16) received the B.E and M.S degrees in electrical engineering from Hohai University, Nanjing, China, in 2009 and 2012, respectively, and the Ph.D. degree in electrical engineering from the University of Hong Kong, Hong Kong, in 2016.

He was a Post-Doctoral Researcher with the University of Hong Kong in 2016, and is currently a Post-Doctoral Researcher with Iowa State University. His research interests include optimization and its applications in power systems,

smart grids, integration of renewable energy sources, and cyber-physical systems.



**Tianguang Lu** (S'16) received the B.S. degree in electrical engineering from Shandong University, Shandong, China, in 2013. He is currently pursuing the Ph.D. degree with the School of Electronic Information and Electrical Engineering, Shanghai Jiaotong University, Shanghai, China.

He was an Electrical Engineer Intern with ABB (China) Inc., Beijing, China, in 2015, and a Visiting Student Researcher with the University of Texas at Arlington, Arlington, TX, USA, and Iowa State University, Ames, IA, USA, in 2016 and 2017,

respectively. His research interests include power distribution systems, microgrids, intelligent algorithms, and renewable energy. Mr. Lu was a recipient of the IEEE Industrial Application Society Prize Paper Award in 2016. His research is currently supported by the National Natural Science Foundation of China and the National Major Research and Development Program of China.

AQ6

AQ7

AQ8

AQ9